Published in The Plant Cell 18, issue 7, 1693-1703, 2006
which should be used for any reference to this work

Plastoglobules Are Lipoprotein Subcompartments of the Chloroplast That Are Permanently Coupled to Thylakoid Membranes and Contain Biosynthetic Enzymes

Jotham R. Austin II,[a,b,1] Elizabeth Frost,[a] Pierre-Alexandre Vidi,[c] Felix Kessler,[c] and L. Andrew Staehelin[a]

[a] Department of Molecular, Cellular, and Developmental Biology, University of Colorado, Boulder, Colorado 80309-0347
[b] Biological Science Division, Office of Shared Research Facilities, University of Chicago, Chicago, Illinois 60637
[c] Université de Neuchâtel, Institut de Botanique, Laboratoire de Physiologie Végétale, CH-2007 Neuchâtel, Switzerland

Plastoglobules are lipoprotein particles inside chloroplasts. Their numbers have been shown to increase during the upregulation of plastid lipid metabolism in response to oxidative stress and during senescence. In this study, we used state-of-the-art high-pressure freezing/freeze-substitution methods combined with electron tomography as well as freeze-etch electron microscopy to characterize the structure and spatial relationship of plastoglobules to thylakoid membranes in developing, mature, and senescing chloroplasts. We demonstrate that plastoglobules are attached to thylakoids through a half-lipid bilayer that surrounds the globule contents and is continuous with the stroma-side leaflet of the thylakoid membrane. During oxidative stress and senescence, plastoglobules form linkage groups that are attached to each other and remain continuous with the thylakoid membrane by extensions of the half-lipid bilayer. Using three-dimensional tomography combined with immunolabeling techniques, we show that the plastoglobules contain the enzyme tocopherol cyclase (VTE1) and that this enzyme extends across the surface monolayer into the interior of the plastoglobules. These findings demonstrate that plastoglobules function as both lipid biosynthesis and storage subcompartments of thylakoid membranes. The permanent structural coupling between plastoglobules and thylakoid membranes suggests that the lipid molecules contained in the plastoglobule cores (carotenoids, plastoquinone, and tocopherol [vitamin E]) are in a dynamic equilibrium with those located in the thylakoid membranes.

INTRODUCTION

Plastoglobules are lipid bodies produced by plastids (Lichtenthaler, 1968). It has been proposed that, like the lipid bodies formed at the endoplasmic reticulum (ER) (Fernandez and Staehelin, 1987), plastoglobules may be surrounded by a lipid monolayer studded with proteins (Kessler et al., 1999; Smith et al., 2000). However, the origin of plastoglobules is still unclear. Whereas some studies have suggested that they form as blebs on thylakoid membranes (Yao et al., 1991a, 1991b; Ghosh et al., 1994) analogous to lipid body formation at the ER (Huang, 1996), others have suggested that they form in conjunction with the inner chloroplast envelope membrane (Kessler et al., 1999). It has also been hypothesized that plastoglobules can detach from their parent membrane and reattach at a different membrane site, potentially ferrying plastid lipids from one site to another (Hansmann and Sitte, 1982).

The number of plastoglobules per plastid has been shown to vary during plastid development. In etioplasts, the number of plastoglobules is high but decreases upon light-induced greening and conversion of the etioplast to chloroplasts (Lichtenthaler and Tevini, 1970; Tevini et al., 1977). During senescence, the number of plastoglobules increases as the thylakoids break down. Plastoglobule numbers also increase in plants subjected to environmental conditions that increase oxidative stress on the photosynthetic apparatus. These include increased concentrations of CO_2 (Sallas et al., 2003), growth in high-copper-containing soil (Panou-Filotheou et al., 2001), drought (Munne-Bosch and Alegre, 2004), increased ozone concentrations (Britvec et al., 2001), high saline concentrations (Sam et al., 2003), exposure to organic Ni(II) complexes (Molas, 2002), viral infection (Hernandez et al., 2004), and microgravity growth conditions (Kochubey et al., 2004).

Biochemical analyses of isolated plastoglobule fractions have shown that they contain a variety of lipidic compounds, including monogalactosyldiacylglycerol, digalactosyldiacylgycerol, free fatty acid, triacylglycerols, carotenoids, prenylquinones (tocopherols, plastoquinone, and menaquinones), and chlorophylls (Lichtenthaler, 1966; Steinmuller and Tevini, 1985; Tevini and Steinmuller, 1985; Ghosh et al., 1994; Kaup et al., 2002). Plastoglobules also contain at least a dozen different proteins (Kessler et al., 1999; Vidi et al., 2006; Ytterberg et al., 2006), but only the plastid lipid-associated proteins, which belong to the PAP/fibrillin family of proteins, have been identified as plastoglobule-specific proteins (Deruere et al., 1994; Pozueta-Romero et al., 1997; Kessler et al., 1999). They have been shown to bind carotenoids and are believed to serve structural roles in both chromoplast carotenoid fibrils and chloroplast plastoglobules

[1] To whom correspondence should be addressed. E-mail jotham@uchicago.edu; fax 773-902-7195.
The author responsible for distribution of materials integral to the findings presented in this article in accordance with the policy described in the Instructions for Authors (www.plantcell.org) is: Jotham R. Austin II (jotham@uchicago.edu).

(Deruere et al., 1994; Kessler et al., 1999; Rey et al., 2000; Laizet et al., 2004). As demonstrated here and elsewhere (Vidi et al., 2006; Ytterberg et al., 2006), there is now evidence for plastoglobules serving a biosynthetic function as well.

To understand how the lipid storage and biosynthetic activities of plastoglobules contribute to the functioning of chloroplasts, it is essential to know where and how plastoglobules are formed and whether they are physically attached to thylakoid membranes during development and senescence. To date, all of the structural studies of plastoglobules have used chemical fixation methods for specimen preparation and transmission electron microscopy for thin-section analyses. These techniques are inherently limited in their ability to preserve and characterize the three-dimensional architecture of these chloroplast components. To surmount these limitations, we have characterized the spatial relationship of plastoglobules and other chloroplast structures using a combination of state-of-the-art electron microscope specimen preparation and analysis techniques, including high-pressure freezing/freeze-substitution, electron tomography, immunoelectron tomography, and freeze-etch electron microscopy methods. Our data demonstrate that plastoglobules form on thylakoid membranes, that they are surrounded by a half bilayer membrane that is continuous with the thylakoid outer leaflet, that they contain different proteins within the lipid monolayer that surrounds them, and that they remain structurally coupled to thylakoids throughout their life span.

RESULTS

Plastoglobules Arise by a Membrane-Blistering Mechanism along Highly Curved Thylakoid Margins

We analyzed 305 plastoglobules contained in 20 tomographic reconstructions (~4500 tomographic slices), ~300 thin-section electron micrographs of chloroplasts preserved by high-pressure

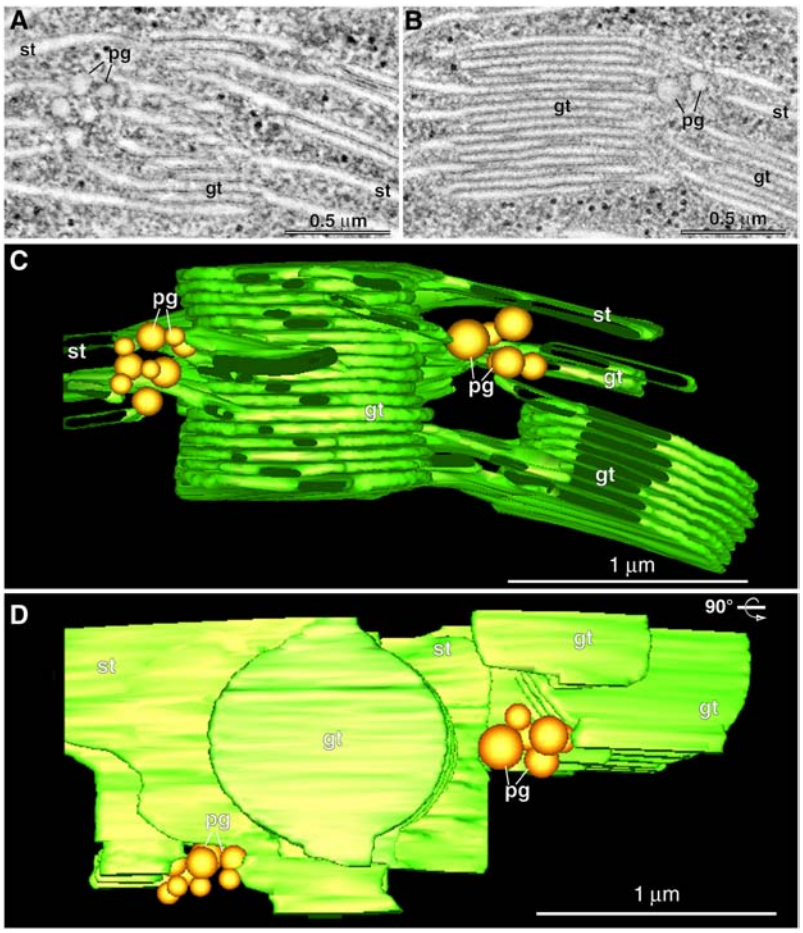

Figure 1. Plastoglobule Location in Relation to the Thylakoid Membranes.

(A) and **(B)** Two composite tomographic slice images (five superimposed serial 2.2-nm slices) of grana thylakoids (gt), stroma thylakoids (st), and plastoglobules (pg) in an intact, isolated spinach chloroplast.

(C) and **(D)** Tomographic model of the grana stack shown in **(A)** and **(B)** as seen in a side view **(C)** and a top-down view **(D)** (**[C]** rotated 90°). Note that in **(D)**, the top-most stoma thylakoid has been removed to provide a clearer view of the clusters of plastoglobules that are associated with areas of high curvature of the stroma and grana thylakoids.

freezing and freeze-substitution techniques, and ~100 electron micrographs of freeze-fractured isolated chloroplasts. To determine whether plastoglobules are formed exclusively in close association with thylakoids, or whether they may arise at the inner chloroplast envelope membrane, we mapped the positions of all of the plastoglobules in our tomograms and thin sections. One hundred percent of the plastoglobules were seen in close proximity to thylakoids, and none was adjacent to an inner envelope membrane (Figures 1 to 4). Furthermore, 98% of the plastoglobules were associated with thylakoid membrane areas with a high curvature (i.e., along the nonappressed thylakoid margins) (Figure 1). The remaining 2% of the plastoglobules were always within 30 nm of such highly curved regions (Figure 2). The highly curved margins of stroma thylakoids also gave rise to more plastoglobules (>70%) than the highly curved, nonappressed regions of grana stacks.

To characterize how plastoglobules are physically linked to the highly curved thylakoid margins, we examined all of the serial 2.2-nm-thick tomographic slices that passed through plastoglobules. The images shown in Figure 2 are from two such series of slice images. Figures 2A to 2C represent images of every fourth 2.2-nm tomographic slice, and Figures 2F to 2H show tilted images of Figure 2E (every seventh 2.2-nm slice image shown). The tomographic reconstruction of the plastoglobule and thylakoid membranes seen in Figures 2A to 2C is illustrated in Figure 2D. Figures 2B and 2G clearly show that the outer leaflet of the thylakoid membrane blistered to generate the plastoglobule, forming a half lipid bilayer cover around the lipidic plastoglobule contents, whereas the inner leaflet of the thylakoid membrane retained its planar configuration.

To confirm these electron tomography data, we also investigated the structures of plastoglobules by means of freeze-fracture (-etch) electron microscopy (Figure 3). The advantage of this technique for analyzing lipidic cellular structures is that the imaging does not depend on any chemical staining of the sample. Instead, the images are produced by platinum-carbon replicas of the rapidly frozen and freeze-fractured (-etched) sample surfaces at −100°C. The most important feature of this technique for this investigation is that at −100°C the fracturing process produces fracture planes that follow interface regions between structures held together by hydrophobic interactions (i.e., along the central plane of the bilayer membrane) (Branton, 1966) and along the interface between the lipid core and the surface monolayer of oil bodies attached to ER membranes (Fernandez and Staehelin, 1987). As demonstrated in Figure 3, the same type of fracture faces seen in oil bodies are also observed in our plastoglobule-containing samples. In particular, in Figures 3A and 3B, the central core region of the plastoglobule is seen to be surrounded by a ridge that corresponds to the edge of the cross-fractured half-lipid bilayers that encompasses the plastoglobules. Similar lipid monolayer structures are seen to form the narrow neck-like region of the two plastoglobules shown in Figure 3D. The micrograph in Figure 3A also demonstrates that the lipid core material of the plastoglobule extends through the neck region to the center of the bilayer membrane (cf. with Figures 2B and 2G). In Figure 3C, the neck region is seen as a funnel-shaped structure with a central lipidic plug caused by the breaking away of the plastoglobule from the neck during the fracturing process.

Single and Grouped Plastoglobules Remain Physically Coupled to Thylakoids throughout Their Life Span

Based on the ultrastructural analysis of chemically fixed chloroplasts and biochemical studies, it has been suggested that

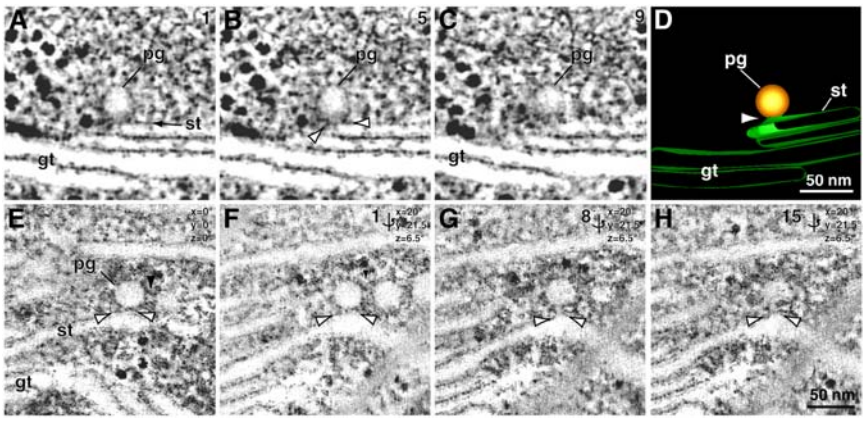

Figure 2. Electron Tomographic Imaging of Plastoglobule–Thylakoid Membrane Connecting Sites.

(A) to **(C)** Serial 2.2-nm tomographic slice images (every fourth slice shown) through a plastoglobule (pg) blistering from the margin of a thylakoid membrane from a greening *Arabidopsis* chloroplast. The arrowheads point to the sites where the outer leaflet of the thylakoid membrane has separated from the inner leaflet to form the half bilayer surrounding the plastoglobule. Note that the inner leaflet of the thylakoid membrane can also be seen in **(B)**. gt, grana thylakoid; st, stroma thylakoid.

(D) Tomographic model of the plastoglobule shown in **(A)** to **(C)**.

(E) A face-on view of a plastoglobule–thylakoid membrane connection.

(F) to **(H)** Serial 2.2-nm rotated ($x = 20°$, $y = 21.5°$, $z = 6.5°$) tomographic slice images of **(E)** through a plastoglobule–thylakoid connection. Note that the arrowheads in **(G)** point to the neck-like plastoglobule–thylakoid membrane continuous membrane connection.

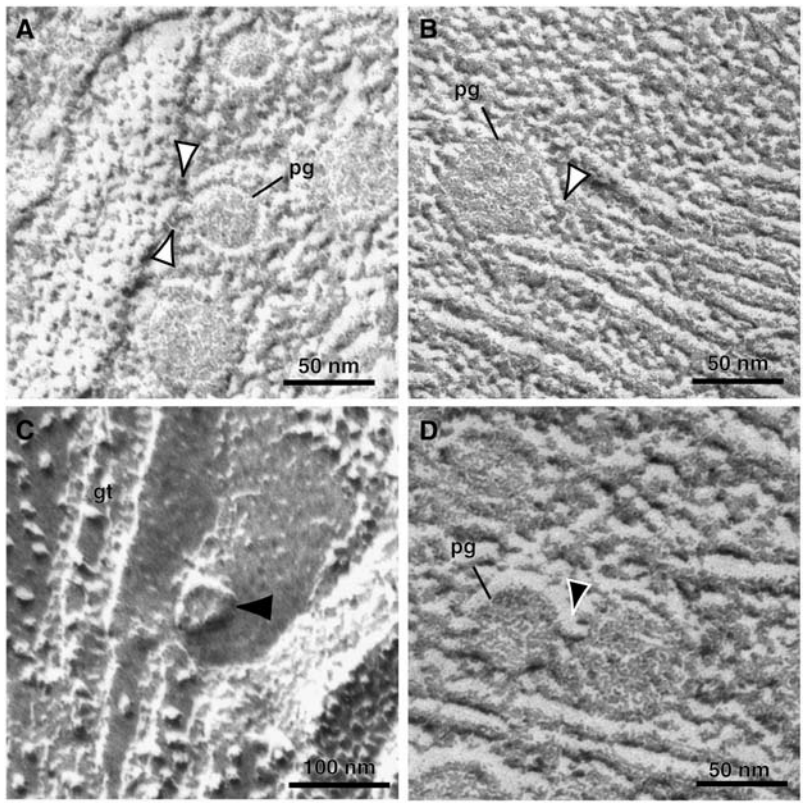

Figure 3. Freeze-Fracture Electron Micrographs of Plastoglobule–Thylakoid and Plastoglobule–Plastoglobule Connections.

(A) and **(B)** Two examples of plastoglobule–thylakoid interactions. In both images, the half-lipid bilayer that surrounds the lipid core has been partly torn away to expose the lipidic contents of the plastoglobule (pg). The edge of the remaining cross-fractured half bilayer is seen as a ridge-like structure that can be followed through the narrow neck region to the stroma leaflet of the thylakoid membrane (arrowheads). The extension of the core material in the neck region up to the middle of the thylakoid membrane is most evident in **(A)** (cf. also with Figure 2G).

(C) The arrowhead points to a cross-fractured neck region exposed by the breaking away of the plastoglobule. The neck region, as seen from the inside of the plastoglobule, exhibits a funnel-shaped geometry.

(D) Longitudinal fracture through two plastoglobules connected through a half-lipid bilayer tube.

plastoglobules develop on thylakoids but may subsequently detach to form free-floating entities (Hansmann and Sitte, 1982). To test this hypothesis, we analyzed >300 plastoglobules in developing, mature, and senescing chloroplasts preserved by high-pressure freezing and freeze-substitution techniques. This analysis failed to detect a single plastoglobule that was free-floating. In fact, using the three-dimensional tomographic serial sectioning tools of IMOD, we determined that even plastoglobules located at a distance from a thylakoid membrane remained physically coupled to the membrane by linking to adjacent plastoglobules via a continuous half bilayer envelope (Figure 4). Examples of the narrow, tubular connecting elements between adjacent plastoglobules are most clearly seen in tomographic images and freeze-fracture micrographs (Figures 3C, 4A, and 4C). Hence, every plastoglobule is always structurally coupled to another plastoglobule and/or to a thylakoid membrane through a half bilayer.

In greening and mature chloroplasts, 95% of the mapped plastoglobules ($n = 50$) were single plastoglobules with diameters of 45 to 60 nm, all of which were coupled to a thylakoid membrane via a narrow, half-lipid bilayer neck (Figures 2, 3A, and 3B). The remaining plastoglobules were organized into small clusters of two or three interconnected plastoglobules (Figures 3C and 4). By contrast, in senescing, light-stressed, and drought-stressed chloroplasts, the plastoglobules not only exhibited greater variations in size (28 to 73 nm in diameter) but also tended to be organized into larger clusters, with as many as seven plastoglobules linked together by a half-lipid bilayer boundary layer (Figures 4C, 4D, and 5). These linked plastoglobules formed both linear aggregates, like beads on a string (Figure 5B), and branched structures, with one plastoglobule connected to either three plastoglobules (Figure 4E) or to two plastoglobules and the thylakoid membrane (Figures 4D and 5D). In the tomographic reconstructions shown in Figures 4 and 5, the sites of the thylakoid-to-plastoglobule links are marked with arrows. Most larger plastoglobule linkage groups exhibit a kinked configuration (Figures 5D and 5E).

PGL35 and Tocopherol Cyclase Localize to the Half Bilayer Surrounding Plastoglobules

Proteomic studies of plastoglobules have shown that they contain structural (PAP/fibrillins) (Kessler et al., 1999) as well as

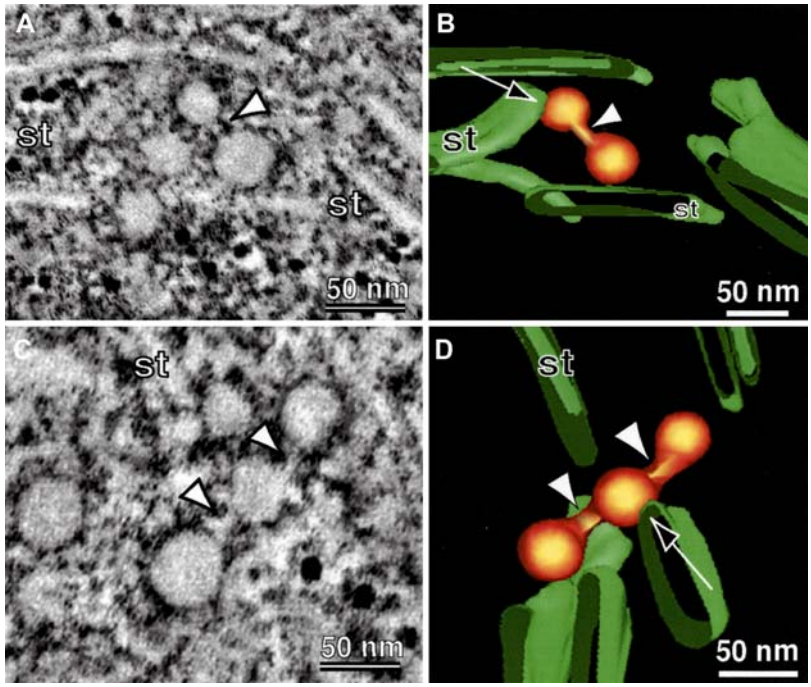

Figure 4. Interconnected Plastoglobules.

Two composite tomographic slice images (**[A]** and **[C]**) (five superimposed serial 2.2-nm slices) of groups of interconnected plastoglobules held together by a common half bilayer surface layer. The image shown in **(A)** and the corresponding tomographic model **(B)** depict two linked plastoglobules in a mature tobacco chloroplast. The image shown in **(C)** and the corresponding tomographic model **(D)** show three interconnected plastoglobules of an isolated intact senescing spinach chloroplast. The white arrowheads point to the links between the interconnected plastoglobules. In both **(B)** and **(D)**, the arrows point to the connecting sites between the plastoglobule and thylakoid membrane. st, stroma thylakoid.

enzymatic proteins (Vidi et al., 2006; Ytterberg et al., 2006). To verify the association of two of these proteins with plastoglobules, we performed immunoelectron tomographic studies on high-pressure frozen/freeze-substituted chloroplasts from *Arabidopsis thaliana*, tobacco (*Nicotiana tabacum*), and spinach (*Spinacia oleracea*) embedded in Lowicryl HM20 resin using specific antibodies raised against two plastoglobulins (pea [*Pisum sativum*] PGL1 [Kessler et al., 1999] and *Arabidopsis* PGL35 [Vidi et al., 2006]) as well as against *Arabidopsis* tocopherol cyclase (VTE1 [Kanwischer et al., 2005]). The anti-PGL1 antibodies were used as controls in all three species to confirm the previous plastoglobule labeling results on chemically fixed isolated pea chloroplast samples by Kessler et al. (1999). In all of our samples, the anti-PGL1 antibodies produced specific labeling of the plastoglobules (data not shown). We examined eight tomographic reconstructions containing 15 anti-VTE1 and 17 anti-PGL35 immunolabeled plastoglobules. Figure 6 shows the labeling of an *Arabidopsis* chloroplast with the anti-PGL35 (Figures 6A to 6D) and the anti-VTE1 (Figures 6E to 6H) antibodies together with corresponding three-dimensional models. Both anti-PGL35 and anti-VTE1 gold particles were bound to the surface of the plastoglobules and to epitopes exposed to the interior of the plastoglobules. This latter type of labeling was made possible by the fact that during the immunolabeling of the thin sections, the hydrophobic lipid core of the plastoglobules can fall out, thereby exposing the inner surface of the plastoglobule half-lipid bilayer. Hence, by exploiting the enhanced *z* axis resolution of the immunotomography techniques, we can determine whether the gold labels are only on the external surface of the plastoglobules or located within the plastoglobule interior (indicating that the proteins are localized within the plastoglobule half-lipid bilayer). As illustrated in Figures 7A to 7E showing an immunolabeled three-dimensional tomogram (every fifth tomographic slice shown), the anti-VTE1 immunogold particles are located at different depths within the plastoglobule (Figure 7F), indicating that VTE1 and PGL35 (data not shown) are anchored within the half-lipid bilayer membrane and extend into the interior of the plastoglobule (Figure 8).

The tomographic models also demonstrated that the anti-PGL35 antibodies labeled the links between connected plastoglobules (data not shown). Both the anti-PGL35 and the anti-VTE1 antibody labeling was limited to the plastoglobules. No labeling was seen over thylakoid or inner envelope membranes.

DISCUSSION

Chloroplasts have been the focus of ultrastructural studies for the past 60 years (Staehelin and Dewit, 1984; Staehelin, 2003). Yet, the formation and spatial organization of plastoglobules present within chloroplasts have remained an enigma. The plastoglobule proteomic study by Kessler et al. (1999) demonstrated that plastoglobules are more than just excess lipid and protein sinks.

However, in the absence of a well-defined structural context, it is difficult to envisage how the different enzymatic activities of plastoglobules relate to chloroplast function. To obtain this ultrastructural information, we reinvestigated the spatial relationship between plastoglobules and thylakoid membranes in samples preserved by high-pressure freezing/freeze-substitution techniques and characterized the structures by a combination of electron tomography, immunoelectron tomography, and freeze-fracture (-etch) methods. Together, these techniques have demonstrated that plastoglobules constitute a distinct structural and functional subcompartment of thylakoids, that they contain both lipid binding proteins and enzymes involved in lipid biosynthesis and metabolism, and that they are always physically coupled to thylakoid membranes via a half-lipid bilayer.

Plastoglobules Are Formed in Regions of High Curvature of Thylakoid Membranes by Blistering of the Outer Membrane Leaflet

The literature on plastoglobules contains conflicting suggestions regarding where they are formed, the inner chloroplast envelope membrane (Kessler et al., 1999) or thylakoids (Ghosh et al., 1994), and the extent to which they can detach and reattach to thylakoids. In this study, we did not observe any plastoglobules attached to or associated with the inner chloroplast envelope membrane or any free-floating plastoglobules in the chloroplast stroma. Indeed, 100% of the ~300 plastoglobules examined were observed to be physically attached to a thylakoid membrane via a half-lipid bilayer

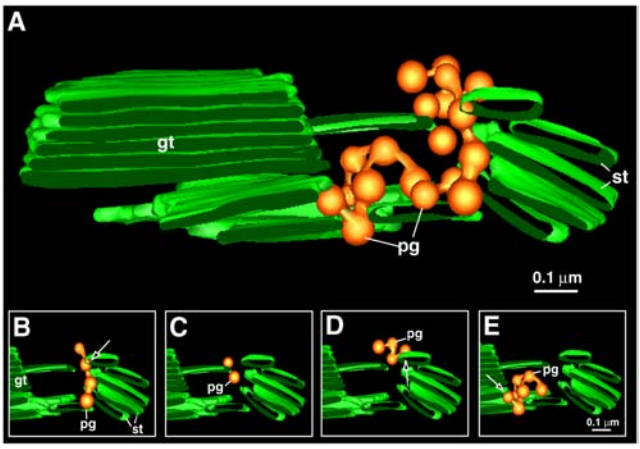

Figure 5. Plastoglobule Cluster.

(A) Tomographic models showing the location and organization of plastoglobules (pg) from an isolated senescing spinach chloroplast. The plastoglobules are associated with areas of high membrane curvature. gt, grana thylakoid; st, stroma thylakoid.

(B) to **(E)** Four groups of interconnected plastoglobules in the large cluster as demonstrated in the following models: four plastoglobules linked linearly **(B)**; two single plastoglobules blistering from a stroma thylakoid membrane **(C)**; four linked plastoglobules in a kinked configuration **(D)**; and seven plastoglobules linked together, also in a kinked configuration **(E)**. Note that in **(B)**, **(D)**, and **(E)**, the arrows point to the connecting sites between the plastoglobule and the thylakoid membrane.

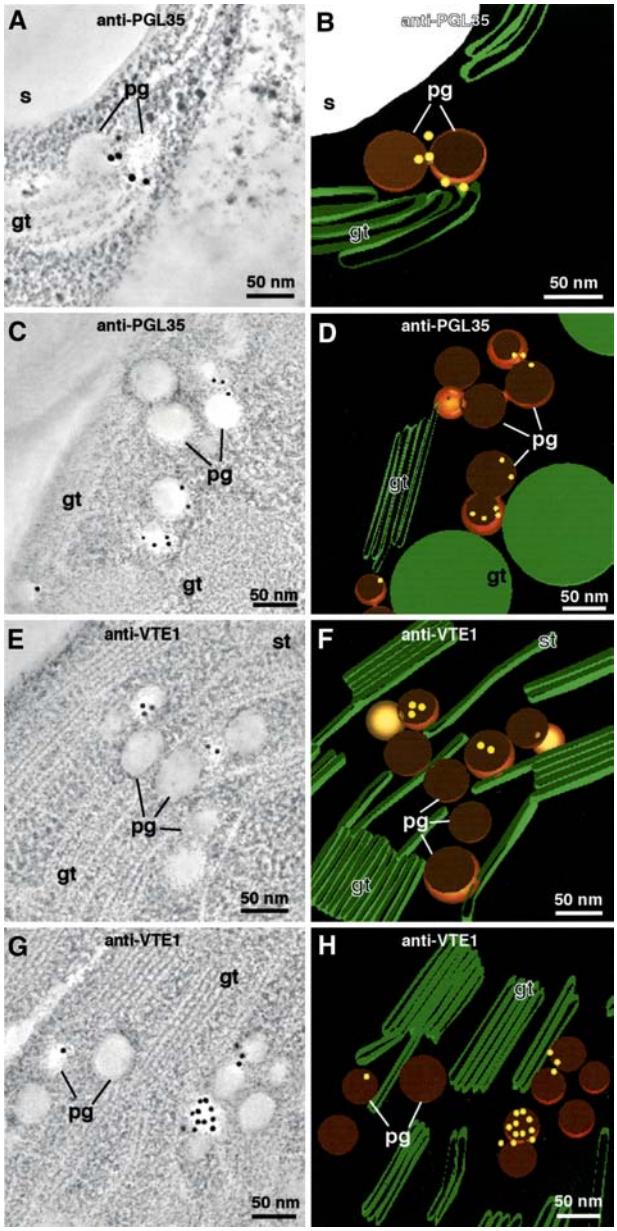

Figure 6. PGL35 and VTE1 Immunogold Labeling.

Tomographic slice image views of plastoglobules in *Arabidopsis* chloroplasts immunolabeled with anti-PGL35 (**[A]** and **[C]**) and anti-VTE1 (**[E]** and **[G]**) antibodies, and corresponding tomographic models depicting the immunogold labels in a three-dimensional context (**[B]** and **[D]** and **[F]** and **[H]**, respectively). The tomographic images are of 20 superimposed 2.2-nm-thick slices. Note that whereas most of the gold label appears to be associated with the coat layer of the cross-sectioned plastoglobules (**[A]** to **[H]**), one of the labeled plastoglobules in **(G)** exhibits labeling across its surface. As demonstrated in Figure 7, this surface corresponds to the inner surface of the plastoglobule coat monolayer. gt, grana thylakoid; pg, plastoglobule; s, starch; st, stroma thylakoid.

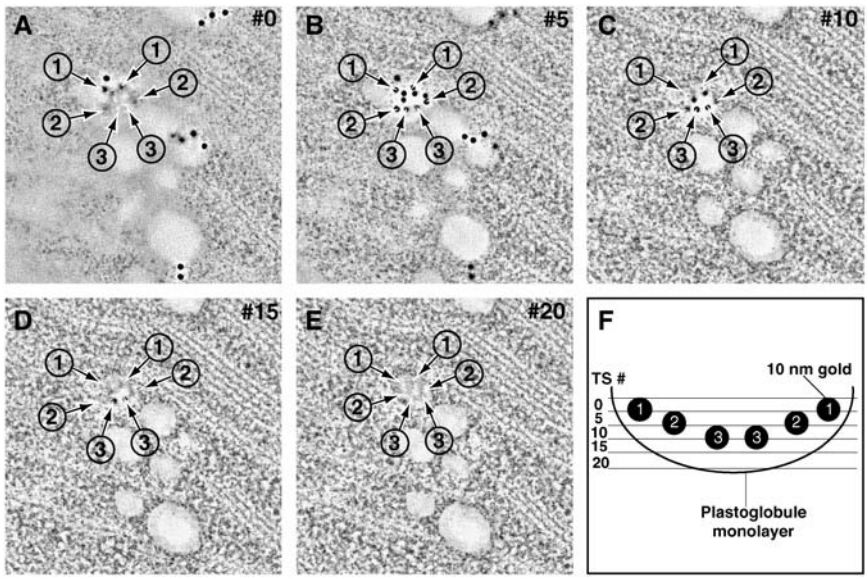

Figure 7. Anti-VTE1 Serial Immunoelectron Tomography.

(A) to **(E)** Serial 2.2-nm tomographic slice images (every fifth slice shown) through a plastoglobule labeled with anti-VTE1. Note that as one proceeds from the top of the section **(A)** to the bottom **(E)**, different groups of 10-nm gold labels, indicated by arrows and numbers, are seen at different depths within the plastoglobule interior.

(F) Cartoon representation of the plastoglobule, as shown in **(A)** to **(E)**, with all of the gold labels (the numbers correspond to the numbers assigned to the gold labels in **[A]** to **[E]**) and their respective positions in each tomographic slice (TS).

that surrounded the lipidic globule core and were continuous with the stroma-side leaflet of the thylakoid membrane (Figures 2B, 2G, 3A, and 8). These observations indicate that plastoglobules remain structurally and functionally coupled to thylakoid membranes throughout their life span.

In light of the results presented here, the similarities between the formation of plastoglobules on thylakoid membranes and the formation of oil bodies on the ER membrane are quite striking. For example, as the triacylglycerol oil molecules are synthesized by ER enzymes, they partition into the interior of the lipid bilayer and accumulate at sites rich in oleosin and other specific molecules (Huang, 1996). During this process, the oleosins induce the cytosolic leaflet of the ER membrane to form a blister that gives rise to a spherical oil body surrounded by a lipid monolayer and the characteristic oil body proteins (Fernandez and Staehelin, 1987; Fernandez et al., 1988). However, unlike the plastoglobules, the oil bodies do appear to detach from the ER membrane, and during seed germination in barley (*Hordeum vulgare*), their phospholipid boundary layer can fuse with the cytosolic leaflet of protein body membranes to allow for the transfer of lipase molecules via lateral diffusion to the oil bodies (Fernandez and Staehelin, 1987).

Plastoglobules Contain Both Structural and Biosynthetic Proteins

One of the most important insights gained from the proteomic analysis of isolated plastoglobules is that they contain, in addition to known structural proteins, enzymes involved in lipid synthesis and metabolism (Vidi et al., 2006; Ytterberg et al., 2006). Members of the structural, carotenoid binding PAP/fibrillin (plastoglobulin) protein family have been shown previously to localize to the surface of plastoglobules (Pozueta-Romero et al., 1997; Kessler et al., 1999). As illustrated in Figures 6A to 6D, we have confirmed this localization in cells preserved by high-pressure freezing/freeze-substitution techniques and immunolabeled with anti-PGL1 and anti-PGL35 antibodies. Of greater interest, however, is the localization of the enzyme tocopherol cyclase (VTE1) to plastoglobules (Figures 6E and 6H). VTE1 catalyzes the penultimate step of tocopherol (vitamin E) synthesis (Kanwischer et al., 2005). It has been shown that tocopherol cyclase activity is increased during oxidative stress, protecting the thylakoid membranes and photosynthetic proteins from oxidative damage caused by activated oxygen species (Porfirova et al., 2002; Kanwischer et al., 2005). Our data show that the anti-VTE1 antibody labeling occurred exclusively over the plastoglobules, thereby confirming that plastoglobules function both as biosynthetic and storage compartments of chloroplasts. The binding of the anti-VTE1 antibodies to the inner surface of the boundary layer of the plastoglobules demonstrates that this enzyme is in contact with the contents of the plastoglobules.

During Periods of Oxidative Stress, the Plastoglobules Become Organized into Large, Interconnected Clusters That Remain Anchored to Thylakoid Membranes

Several environmental and developmental conditions have been shown to increase plastoglobule numbers and produce plastoglobule clusters in chloroplasts, including oxidative stress,

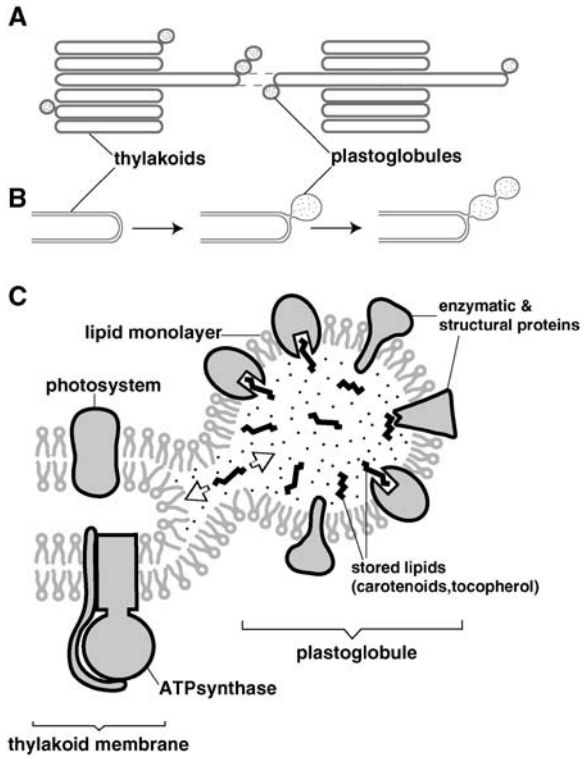

Figure 8. Plastoglobule Formation and Organization Overview.

(A) Plastoglobules form exclusively on thylakoid membranes at areas of high curvature.

(B) Plastoglobules blister from the outer leaflet of the thylakoid membrane, and this half-lipid bilayer surrounds the plastoglobule. Mostly under oxidative stress conditions, the plastoglobules form interconnected linkage groups surrounded by a single continuous half-lipid bilayer.

(C) The half-lipid bilayer that surrounds the plastoglobule is studded with several proteins, both structural (plastoglobulins) and enzymatic (VTE1). These proteins would have their functional sites located within the plastoglobule interior.

senescence, and the chloroplast-to-chromoplast transition (Sprey and Lichtenthaler, 1966; Lichtenthaler, 1968; Weinert, 1970; Steinmuller and Tevini, 1985; Deruere et al., 1994; Smith et al., 2000). Because these conditions also lead to increases in plastoglobule-specific proteins, including VTE1 (Porfirova et al., 2002; Kanwischer et al., 2005) and PAP/fibrillins (Bathgate et al., 1985; Deruere et al., 1994), it has been suggested that plastoglobule formation is dependent on the synthesis of such proteins. This notion has been tested by expressing the pepper (*Capsicum annuum*) fibrillin protein in tobacco, yielding plants with increased numbers of clustered plastoglobules within the chloroplasts (Rey et al., 2000). Despite numerous reports on plastoglobule clustering, neither the origin nor the functional significance of the clustering process has been addressed.

The discovery that the clustered plastoglobules formed under stress conditions are structurally linked to each other and to thylakoid membranes via an encompassing lipid monolayer (Figures 3 and 4) provides new insights into both the mechanism of plastoglobule formation and their function. First, it suggests that plastoglobules can be formed by two mechanisms: through blistering of the stroma leaflet of thylakoid membranes (primary blistering events) and by blistering from the surface of existing plastoglobules (secondary blistering events). Furthermore, the maintenance of the connections between the plastoglobules and the thylakoid membranes suggests that the plastoglobules remain functionally coupled to thylakoids throughout their life span. Most notably, the type of physical coupling observed allows for the free exchange of lipid molecules such as plastoquinone, carotenoids, and tocopherol (vitamin E) between the plastoglobules, the sites of their synthesis and/or storage, and the thylakoids, where these molecules serve as electron carriers and protect the complexes of the photosynthetic apparatus from free radical damage.

Plastoglobule Formation Appears to Be Driven by the Physicochemical Properties of Plastoglobulin-Type Proteins

Our anti-PGL35 labeling shows that PGL35 is confined to the surface layer of plastoglobules (Figure 6) and that it is not found to any significant extent in either thylakoid membranes or the chloroplast stroma. This finding supports an earlier study in which the related plastoglobulin PGL1 was found to be exposed on the surface of plastoglobules (Kessler et al., 1999). Plastoglobulins have also been shown to bind carotenoids, hydrophobic molecules that partition into the interior of bilayer membranes (Deruere et al., 1994; Kessler et al., 1999; Laizet et al., 2004). Together with our immunotomography data, these findings suggest that plastoglobulins are iceberg- or thumbtack-type molecules with a hydrophilic domain exposed to the chloroplast stroma and a hydrophobic domain that extends into the interior of the plastoglobules and is involved in carotenoid binding (Figure 8). Thus, plastoglobulins appear to possess architectural features reminiscent of oleosin molecules, which have been shown to induce the membrane-blistering process that gives rise to lipid bodies on the ER and also to stabilize the lipid bodies formed in this manner (reviewed in Murphy, 1993). Based on these similarities, we postulate that plastoglobulins share the ability of oleosins to induce blister formation on thylakoid membranes in response to the accumulation of protective hydrophobic molecules such as carotenoids, tocopherol, and plastoquinone in these membranes.

The extent to which enzymes such as VTE1 also participate in the generation of new plastoglobules is unknown. The observation that VTE1 extends beyond the inner surface of the half bilayer boundary layer and into the plastoglobule core (Figure 7) is supportive of the idea that this protein could be involved in plastoglobule formation. As with PGL35, this finding also suggests that the active site of VTE1 is located within the lipidic core of plastoglobules and that the protein extends to the outer surface of the plastoglobule.

The observation that virtually all (~98%) of the plastoglobules were connected to the highly curved margins of the thylakoids suggests that the physical properties and/or composition of these curved membrane regions are conductive to plastoglobule formation. In particular, the packing geometry of the bilayer lipids in such curved regions (Figure 8) would favor the accumulation of wedge-shaped integral proteins, such as plastoglobulins and

VTE1, but not bilayer-spanning membrane proteins, such as the complexes of the photosynthetic electron transport chain (Merchant and Sawaya, 2005).

METHODS

Plant Material

Seeds of *Arabidopsis thaliana* (Landsberg *erecta* wild type) and tobacco (*Nicotiana tabacum*) were planted on 0.8% (w/v) agar plates with Murashige and Skoog medium and 1% sucrose for 5 d. Plants were grown at a temperature of 23°C, a light intensity of 150 $\mu mol \cdot m^{-2} \cdot s^{-1}$, and a photoperiod of 16/8 h light/dark. Soil-grown plants under high light stress were grown under 700 $\mu mol \cdot m^{-2} \cdot s^{-1}$, and drought stress was induced by watering plants once weekly. Fresh spinach (*Spinacia oleracea*) was bought at a local supermarket (Whole Foods Market) and used the same day.

Intact Chloroplast Isolation for Electron Microscopy

Fifty grams of washed spinach leaves was added to 125 mL of buffer 1 (0.4 M NaCl, 2 mM MgCl, 0.2% BSA, and 20 mM Tricine, pH 8.0) and diced in a blender equipped with razor blades. This was filtered through four layers of cheesecloth, and large debris was removed by centrifuging at 300*g* for 1 min. The supernatant was centrifuged at 4000*g* to pellet chloroplasts. The resulting pellet of chloroplast was washed gently, without disrupting the pellet, with buffer 2 (0.15 M NaCl, 5 mM MgCl, 0.2% BSA, and 20 mM Tricine, pH 8.0), and the supernatant was removed and replaced with buffer 3 (0.4 M sucrose, 0.15 M NaCl, 5 mM MgCl, and 20 nM HEPES, pH 7.5).

Sample Preparation for Electron Tomography

Leaves were excised from plants and transferred to aluminum sample holders cryoprotected with 150 mM sucrose, or isolated chloroplasts were placed into aluminum sample holders and frozen in a Baltec HPM 010 high-pressure freezer (Technotrade). Samples were then freeze-substituted in 2% OsO_4 in anhydrous acetone at −80°C for 5 d, followed by slow warming to room temperature over a period of 2 d, removed from the holders, and infiltrated with increasing concentrations of Epon (Ted Pella). Polymerization was performed at 60°C for 2 d under vacuum. Epon sections (250 to 450 nm thick) were prepared for electron tomography as described by Otegui et al. (2001).

For protein immunogold labeling, the high-pressure frozen samples were substituted in 0.1% uranyl acetate plus 0.25% glutaraldehyde in acetone at −80°C for 5 d and then warmed to −60°C for 18 h. After several acetone rinses, samples were removed from the holders and slowly infiltrated under controlled time and temperature conditions in a Leica AFS system at −60°C with Lowicryl HM20 resin according to the following schedule: 25, 50, 75, and 100% (12 h at each concentration). The samples were finally polymerized at −60°C under UV light for 72 h. During an additional 3 d, 100% HM20 was used and was replaced with freshly made resin every 8 h.

Immunocytochemistry

The antibodies pea (*Pisum sativum*) anti-PG1 (Kessler et al., 1999), *Arabidopsis* anti-PGL35 (Vidi et al., 2006), and *Arabidopsis* anti-VTE1 (Kanwischer et al., 2005) were used to determine whether these proteins were specific to plastoglobules. Samples embedded in Lowicryl HM20 were sectioned into 100-nm-thick sections and placed on Formvar-coated gold slot grids. Immunocytochemistry was performed essentially as described by Otegui et al. (2001). Briefly, the sections were blocked for 20 min with a 5% (w/v) solution of nonfat milk in TBS plus 0.1% Tween 20 (TBST). Primary antibodies were diluted 1:20 in a solution of 2.5% nonfat milk in TBST at room temperature for 1 h. The sections were rinsed in a stream of TBS plus 0.5% Tween 20 and then transferred to the secondary antibody (anti-rabbit IgG 1:20 in TBST) conjugated to 10-nm gold particles for 1 h. Control procedures were performed by omitting the primary antibody.

Freeze-Fracture

Isolated intact chloroplasts were prepared as described above. After the 300*g* spin, the supernatant was pelleted at 1000*g*, the chloroplasts were resuspended in buffer 3 and pelleted at 10,000*g*, and the pelleted material was rapidly frozen on copper supports in liquid propane held at ~−160°C. Preparation of the freeze-fracture replicas was according to Greene et al. (1988).

Intermediate- and High-Voltage Electron Microscopy and Acquisition of Tilt Series Images

Seventeen tomograms were collected on a FEI Tecnai TF30 intermediate-voltage electron microscope operating at 300 kV. The images were taken at ×20,000 from +60°C to −60°C at 1°C intervals about two orthogonal axes (Ladinsky et al., 1997) and collected with a Gatan Megascan 795 digital camera that covered an area of 2.6 × 2.6 μm^2 and had a resolution of 2048 × 2048 pixels at a pixel size of 1.26 nm. The remaining tomograms were collected on a JEM-1000 high-voltage electron microscope (JEOL) operating at 750 kV. The images were collected as described by Austin et al. (2005).

Three-Dimensional Tomographic Reconstruction, Modeling, and Analysis

The images (single or montaged frames) were aligned using the gold particles as fiducial markers as described previously (Ladinsky et al., 1999). Each set of aligned tilts was reconstructed into a single-axis tomogram using the R-weighted back-projection algorithm (Gilbert, 1972). Merging the two single-axis tomograms into a dual-axis tomogram involved a warping procedure rather than a single linear transformation producing the dual-axis tomogram (Mastronarde, 1997). In addition, dual-axis tomograms computed from adjacent serial sections were aligned and joined to increase the reconstructed volume (Austin et al., 2005). Tomograms were displayed and analyzed with 3dmod, the graphics component of the 3DMOD (formerly IMOD) software package (Kremer et al., 1996). Membranous structures, microtubules, and all types of vesicles were modeled as described previously (Marsh et al., 2001). Once a model was completed, meshes of triangles were computed to define the surface of each object (Kremer et al., 1996).

The image-slicer tool of 3DMOD was used to display and analyze tomographic slices extracted from the tomogram in any position or tilt around the *x*, *y*, or *z* axis. This tool allowed us to obtain squeezed images in which a number of consecutive 2.2-nm tomographic slices were combined, thus generating *z* projections of different thicknesses, more similar to conventional electron microscopy thin sections.

ACKNOWLEDGMENTS

We thank Byung-Ho Kang and Bryon S. Donohoe for helpful conversations about this work. David Mastronarde and Richard Gaudette provided essential application software and support. We also thank Peter Dörmann for the anti-VTE1 antibodies. F.K. and P.-A.V. were supported by the National Centers of Competence in Research Plant Survival Project. This work was supported by USDA, Cooperative State Research, Education, and Extension Service, Grant 2003-02588 to J.R.A.

Received November 28, 2005; revised March 21, 2006; accepted May 2, 2006; published May 26, 2006.

REFERENCES

Austin, J.R., Segui-Simarro, J.M., and Staehelin, L.A. (2005). Quantitative analysis of changes in spatial distribution and plus-end geometry of microtubules involved in plant-cell cytokinesis. J. Cell Sci. **118,** 3895–3903.

Bathgate, B., Purton, M.E., Grierson, D., and Goodenough, P.W. (1985). Plastid changes during the conversion of chloroplasts to chromoplasts in ripening tomatoes. Planta **165,** 197–204.

Branton, D. (1966). Fracture faces of frozen membranes. Proc. Natl. Acad. Sci. USA **55,** 1048–1050.

Britvec, M., Reichenauer, T., Soja, G., Ljubesic, N., Eid, M., and Pecina, M. (2001). Ultrastructure changes in grapevine chloroplasts caused by increased tropospheric ozone concentrations. Biologia (Bratisl.) **56,** 417–424.

Deruere, J., Romer, S., d'Harlingue, A., Backhaus, R.A., Kuntz, M., and Camara, B. (1994). Fibril assembly and carotenoid overaccumulation in chromoplasts—A model for supramolecular lipoprotein structures. Plant Cell **6,** 119–133.

Fernandez, D.E., Qu, R.D., Huang, A.H.C., and Staehelin, L.A. (1988). Immunogold localization of the L3 protein of maize lipid bodies during germination and seedling growth. Plant Physiol. **86,** 270–274.

Fernandez, D.E., and Staehelin, L.A. (1987). Does gibberellic-acid induce the transfer of lipase from protein bodies to lipid bodies in barley aleurone cells? Plant Physiol. **85,** 487–496.

Ghosh, S., Hudak, K.A., Dumbroff, E.B., and Thompson, J.E. (1994). Release of photosynthetic protein catabolites by blebbing from thylakoids. Plant Physiol. **106,** 1547–1553.

Gilbert, P.F. (1972). The reconstruction of a three-dimensional structure from projections and its application to electron microscopy. II. Direct methods. Proc. R. Soc. Lond. B Biol. Sci. **182,** 89–102.

Greene, B.A., Staehelin, L.A., and Melis, A. (1988). Compensatory alterations in the photochemical apparatus of a photoregulatory, chlorophyll-B-deficient mutant of maize. Plant Physiol. **87,** 365–370.

Hansmann, P., and Sitte, P. (1982). Composition and molecular structure of chromoplast globules of *Viola tricolor.* Plant Cell Rep. **1,** 111–114.

Hernandez, J.A., Rubio, M., Olmos, E., Ros-Barcelo, A., and Martinez-Gomez, P. (2004). Oxidative stress induced by long-term plum pox virus infection in peach (*Prunus persica*). Physiol. Plant. **122,** 486–495.

Huang, A.H.C. (1996). Oleosins and oil bodies in seeds and other organs. Plant Physiol. **110,** 1055–1061.

Kanwischer, M., Porfirova, S., Bergmuller, E., and Dormann, P. (2005). Alterations in tocopherol cyclase activity in transgenic and mutant plants of Arabidopsis affect tocopherol content, tocopherol composition, and oxidative stress. Plant Physiol. **137,** 713–723.

Kaup, M.T., Froese, C.D., and Thompson, J.E. (2002). A role for diacylglycerol acyltransferase during leaf senescence. Plant Physiol. **129,** 1616–1626.

Kessler, F., Schnell, D., and Blobel, G. (1999). Identification of proteins associated with plastoglobules isolated from pea (*Pisum sativum* L.) chloroplasts. Planta **208,** 107–113.

Kochubey, S.M., Adamchuk, N.I., Kordyum, E.I., and Guikema, J.A. (2004). Microgravity affects the photosynthetic apparatus of *Brassica rapa* L. Plant Biosyst. **138,** 1–9.

Kremer, J.R., Mastronarde, D.N., and McIntosh, J.R. (1996). Computer visualization of three-dimensional image data using IMOD. J. Struct. Biol. **116,** 71–76.

Ladinsky, M.S., Kremer, J.R., Mastronarde, D.N., McIntosh, J.R., Staehelin, L.A., and Howell, K.E. (1997). HVEM tomography of the Golgi ribbon in cryofixed NRK cells: The non-compact region, the CGN and TGN. Mol. Biol. Cell **8,** 2040.

Ladinsky, M.S., Marsh, B.J., Mastronarde, D.N., McIntosh, J.R., and Howell, K.E. (1999). Temperature perturbation and cisternal maturation: Evidence for increased cisternal volume, not cisternal number. Mol. Biol. Cell **10,** 114a.

Laizet, Y., Pointer, D., Mache, R., and Kuntz, M. (2004). Subfamily organization and phylogenetic origin of genes encoding plastid lipid-associated proteins of the fibrillin type. Genome Sci. Technol. **3,** 19–28.

Lichtenthaler, H.K. (1966). Plastoglobuli und Plastidenstruktur. Ber. Dtsch. Bot. Ges. **79,** 82–88.

Lichtenthaler, H.K. (1968). Plastoglobuli and fine structure of plastids. Endeavour **27,** 144–148.

Lichtenthaler, H.K., and Tevini, M. (1970). Distribution of pigments, plastid quinones and plastoglobuli in different particle fractions obtained from sonicated spinach chloroplasts. Z. Pflanzenphysiol. **62,** 33–39.

Marsh, B.J., Mastronarde, D.N., Buttle, K.F., Howell, K.E., and McIntosh, J.R. (2001). Organellar relationships in the Golgi region of the pancreatic beta cell line, HIT-T15, visualized by high resolution electron tomography. Proc. Natl. Acad. Sci. USA **98,** 2399–2406.

Mastronarde, D.N. (1997). Dual-axis tomography: An approach with alignment methods that preserve resolution. J. Struct. Biol. **120,** 343–352.

Merchant, S., and Sawaya, M.R. (2005). The light reactions: A guide to recent acquisitions for the picture gallery. Plant Cell **17,** 648–663.

Molas, J. (2002). Changes of chloroplast ultrastructure and total chlorophyll concentration in cabbage leaves caused by excess of organic Ni(II) complexes. Environ. Exp. Bot. **47,** 115–126.

Munne-Bosch, S., and Alegre, L. (2004). Die and let live: Leaf senescence contributes to plant survival under drought stress. Funct. Plant Biol. **31,** 203–216.

Murphy, D.J. (1993). Structure, function and biogenesis of storage lipid bodies and oleosins in plants. Prog. Lipid Res. **32,** 247–280.

Otegui, M.S., Mastronarde, D.N., Kang, B.H., Bednarek, S.Y., and Staehelin, L.A. (2001). Three-dimensional analysis of syncytial-type cell plates during endosperm cellularization visualized by high resolution electron tomography. Plant Cell **13,** 2033–2051.

Panou-Filotheou, H., Bosabalidis, A.M., and Karataglis, S. (2001). Effects of copper toxicity on leaves of oregano (*Origanum vulgare* subsp *hirtum*). Ann. Bot. (Lond.) **88,** 207–214.

Porfirova, S., Bergmuller, E., Tropf, S., Lemke, R., and Dormann, P. (2002). Isolation of an Arabidopsis mutant lacking vitamin E and identification of a cyclase essential for all tocopherol biosynthesis. Proc. Natl. Acad. Sci. USA **99,** 12495–12500.

Pozueta-Romero, J., Rafia, F., Houlne, G., Cheniclet, C., Carde, J.P., Schantz, M.L., and Schantz, R. (1997). A ubiquitous plant housekeeping gene, PAP, encodes a major protein component of bell pepper chromoplasts. Plant Physiol. **115,** 1185–1194.

Rey, P., Gillet, B., Romer, S., Eymery, F., Massimino, J., Peltier, G., and Kuntz, M. (2000). Over-expression of a pepper plastid lipid-associated protein in tobacco leads to changes in plastid ultrastructure and plant development upon stress. Plant J. **21,** 483–494.

Sallas, L., Luomala, E.M., Utriainen, J., Kainulainen, P., and Holopainen, J.K. (2003). Contrasting effects of elevated carbon dioxide concentration and temperature on Rubisco activity, chlorophyll fluorescence, needle ultrastructure and secondary metabolites in conifer seedlings. Tree Physiol. **23,** 97–108.

Sam, O., Ramirez, C., Coronado, M.J., Testillano, P.S., and Risueno, M.C. (2003). Changes in tomato leaves induced by NaCl stress: Leaf organization and cell ultrastructure. Biol. Plant. **47,** 361–366.

Smith, M.D., Licatalosi, D.D., and Thompson, J.E. (2000). Co-association of cytochrome f catabolites and plastid-lipid-associated protein with chloroplast lipid particles. Plant Physiol. **124,** 211–221.

Sprey, B., and Lichtenthaler, H.K. (1966). Zur Frage der Beziehungen Zwischen Plastoglobuli und Thylakoidgenese in Gerstenkeimlingen. Z. Naturforsch. Teil B Chem. Biochem. Biophys. Biol. Verwandten Gebiete **B21,** 697–699.

Staehelin, L.A. (2003). Chloroplast structure: From chlorophyll granules to supra-molecular architecture of thylakoid membranes. Photosynth. Res. **76,** 185–196.

Staehelin, L.A., and Dewit, M. (1984). Correlation of structure and function of chloroplast membranes at the supramolecular level. J. Cell. Biochem. **24,** 261–269.

Steinmuller, D., and Tevini, M. (1985). Composition and function of plastoglobuli. I. Isolation and purification from chloroplasts and chromoplasts. Planta **163,** 201–207.

Tevini, M., Herm, K., and Leonhardt, H.D. (1977). Lipids and function of etiochloroplasts after UV, blue and red light illumination. Biochem. Soc. Trans. **5,** 95–98.

Tevini, M., and Steinmuller, D. (1985). Composition and function of plastoglobuli. II. Lipid composition of leaves and plastoglobuli during beech leaf senescence. Planta **163,** 91–96.

Vidi, P.-A., Kanwischer, M., Baginsky, S., Austin, J.R., Csucs, G., Dormann, P., Kessler, F., and Brehelin, C. (2006). Tocopherol cyclase (VTE1) localization and vitamin E accumulation in chloroplast plastoglobule lipoprotein particles. J. Biol. Chem. **281,** 11225–11234.

Weinert, H.J. (1970). Semigroups of right quotients of topological semigroups. Trans. Am. Math. Soc. **147,** 333–339.

Yao, K., Paliyath, G., Humphrey, R.W., Hallett, F.R., and Thompson, J.E. (1991a). Identification and characterization of nonsedimentable lipid protein microvesicles. Proc. Natl. Acad. Sci. USA **88,** 2269–2273.

Yao, K.N., Paliyath, G., and Thompson, J.E. (1991b). Nonsedimentable microvesicles from senescing bean cotyledons contain gel phase-forming phospholipid degradation products. Plant Physiol. **97,** 502–508.

Ytterberg, A.J., Peltier, J.B., and van Wijk, K.J. (2006). Protein profiling of plastoglobules in chloroplasts and chromoplasts. A surprising site for differential accumulation of metabolic enzymes. Plant Physiol. **140,** 984–997.